A High-Sensitivity CMOS-Compatible Biosensing System Based on Absorption Photometry

Yu-Wei Chang, Ping-Chun Yu, Yang-Tung Huang, *Member, IEEE*, and Yuh-Shyong Yang

***Abstract*—An optical biosensing system based on a standard CMOS technology and absorption photometry is proposed. Within the compact prototype, a CMOS sensor consisting a P^+/N_{well} finger photodiode and a transimpedance amplifier was implemented in a standard 0.35-μm CMOS technology. The ABTS/H_2O_2/HRP method was adopted to be coupled with various analytes of interest, such as glucose and histamine, which can serve as the basis for medical diagnosis. The experimental results demonstrate that the minimum concentrations successfully detected for H_2O_2, glucose, and histamine are 1 μM, 1 μM, and 10 μM, respectively. The detection limits are at least one order of magnitude better than those of reported CMOS biosensors, and are even comparable to those of a commercial spectrophotometer.**

***Index Terms*—Biomedical transducers, CMOS analog integrated circuits, medical diagnosis, optical receivers.**

I. Introduction

With the rapid progress of biotechnology and microelectronics, a new generation of biomedical diagnosis is expected worldwide. The development of a portable, accurate, inexpensive, and easy-to-use biosensor has become the most important niche in the health care industry [1], [2]. Detecting the optical properties changed by chemical reactions is a competent approach to examine various important biological molecules [3], [4].

Among the optical biosensing techniques, emission photometry and absorption photometry have drawn substantial attention in the area of medical diagnosis [1]–[9]. Emission photometry is the detection of the light emitted by molecules through chemical reactions in response to the concentration of an analyte. The light emission process can further be classified into chemiluminescence, fluorescence, and phosphorescence according to specific characteristics. This popular technique is capable of real-time measurement with high selectivity to the analyte. However, it may suffer from luminophor degeneration, which leads to signal attenuation with time [4]–[8]. Circumventing this difficulty, absorption photometry, another widely used technique, relies on the change of photon absorption through chemical reactions in response to the analyte concentration. The biosensing system based on absorption photometry offers advantages for analyte monitoring with high spatial resolution and has potential for applications in microarray analysis [4], [9].

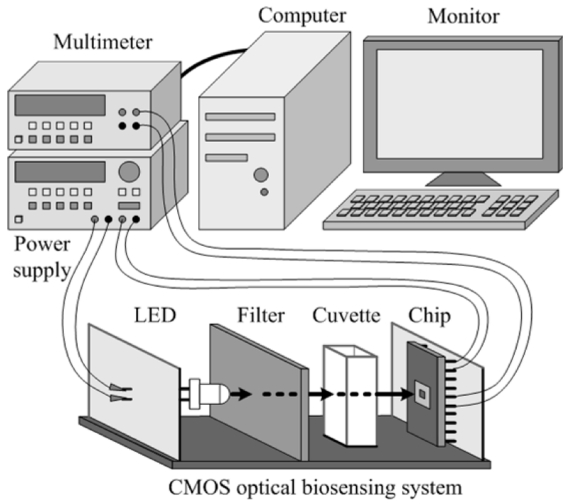

Fig. 1. The diagram of the miniature CMOS optical biosensing system and the experimental setup.

Regarding the commercial instruments for optical analysis, a photomultiplier tube usually serves as the optical sensor in a spectrophotometer. Commonly used wavelength range includes ultraviolet and visible light. Despite its high sensitivity, the spectrophotometer has limited applications in home care instruments because of its bulky size, high cost, and high voltage (about 1000 V) [10]. On the other hand, the CMOS photodetector is characterized as having a small size, a low cost, a high throughput, and low power consumption. Hence, it becomes an attractive candidate for personalized diagnostic kits. Although much research has been devoted to CMOS biosensor using emission photometry, few studies have been done on CMOS biosensor using absorption photometry.

Based on a standard CMOS technology and absorption photometry, an optical biosensing system with a high sensitivity and real-time measurement capability is proposed [11]. The whole system was assembled into a compact prototype, and has great potential toward a practical home care instrument for personalized clinical diagnosis.

II. Principles and Methods

A. System Sketch

The diagram of the proposed CMOS optical biosensing system is illustrated in Fig. 1. A narrowband light emitting

Manuscript received March 12, 2008; revised May 26, 2008; accepted June 02, 2008. Current version published January 09, 2009. This work was supported in part by the MoE ATU plan. The associate editor coordinating the review of this paper and approving it for publication was Prof. Michael Schoening.

Y.-W. Chang is with the Department of Engineering and the Institute of Electronics, National Chiao Tung University, Hsinchu City 300, Taiwan (e-mail: jameschang.ee93g@nctu.edu.tw).

P.-C. Yu and Y.-S. Yang are with the Department Biological Science and Technology, National Chiao Tung University, Hsinchu City 300, Taiwan (e-mail: gbu4806@yahoo.com.tw; ysyang@mail.nctu.edu.tw).

Y.-T. Huang is with the Department of Electronics Engineering, Institute of Electronics, and the Department of Biological Science and Technology, National Chiao Tung University, Hsinchu City 300, Taiwan (e-mail: huangyt@cc.nctu.edu.tw).

Digital Object Identifier 10.1109/JSEN.2008.2011079

diode (LED) is used as the light source, and a bandpass filter allows the light of a specific wavelength to travel through the cuvette, in which the light is modulated by the biochemical materials. The light after passing through the cuvette is detected by the CMOS biochip, which is mainly composed of a photodetector and a transimpedance amplifier (TIA). The photodetector converts the modulated optical signals into current signals, and then the TIA converts them into voltage signals. The voltage signals are measured by a multimeter (Agilent 34401A), which is connected to a personal computer via a general purpose interface bus (GPIB), and an application software (Labview) is used for data acquisition.

B. Biochemical Reactions

In this study, the ABTS/H_2O_2/HRP method is adopted as the basis for biomedical applications. The biochemical equation is expressed as [12]

$$\mathrm{ABTS} + \mathrm{H_2O_2} \xrightarrow{\mathrm{HRP}} \mathrm{ABTS^+} + \mathrm{H_2O} \tag{1}$$

where ABTS represents 2,2'-azino-bis(3-ethylbenzthiazoline-6-sulphonic acid), and HRP stands for horseradish peroxidase. For qualitative analysis, one can easily observe this chemical reaction since the ABTS solution is visually light green and the $ABTS^+$ solution is dark blue. For quantitative analysis, one can detect the optical absorbance of the solution to evaluate the concentration. The absorption spectra obtained from a standard spectrophotometer (Hitachi U-3310) show that ABTS has an absorption peak at 340 nm with 50-nm FWHM (full width at half maximum), whereas $ABTS^+$ has an absorption peak at 415 nm with 50-nm FWHM and lower broad peaks at 640 and 730 nm with 340-nm FWHM.

The absorbance A of the materials is described by the Beer–Lambert law [3]

$$A = -\log\left(\frac{I}{I_0}\right) = \epsilon_\lambda \cdot l \cdot c \Longrightarrow A \propto c \tag{2}$$

where I_0 and I, respectively, denote the initial light intensity and the light intensity after passing through the material, ϵ_λ is the wavelength-dependent molar absorptivity in units of $1 \cdot \mathrm{mol}^{-1} \cdot \mathrm{cm}^{-1}$, l is the path length in units of cm, and c is the concentration of absorbing species in the material in units of $\mathrm{mol} \cdot \mathrm{l}^{-1}$. With a monochromatic light source and a fixed path length, the absorbance would be proportional to the analyte concentration. Thereby detecting the optical signals modulated by the biochemical reactions is an efficient way to quantitate H_2O_2.

For the ABTS/H_2O_2/HRP method, the initial rate v of the overall reaction is expressed as [13]

$$v = \frac{dA}{dt} = \frac{V_{\max} \cdot [\mathrm{H_2O_2}]}{[\mathrm{H_2O_2}] + K_m} \Longrightarrow v \propto \mathrm{small}\ [\mathrm{H_2O_2}] \tag{3}$$

where $V_{\max}$ represents the maximum reaction rate, $[H_2O_2]$ represents H_2O_2 concentration, and K_m represents the Michaelis constant (defined as the H_2O_2 concentration at which the reaction occurs at half of the maximum rate.) K_m is an indicator showing the affinity between an enzyme and a given substrate; at the same time it further reveals the stability of the enzyme-substrate complex. Referring to (3), while $[H_2O_2]$ is relatively smaller than K_m, the initial rate v would be approximately proportional to $[H_2O_2]$.

Moreover, many important biomedical targets such as glucose, histamine, lactate, and uric acid, can be successfully catalyzed to H_2O_2 by different enzymes. The biochemical reactions for glucose and histamine can be expressed as [14]

$$\mathrm{Glucose} + \mathrm{O_2} \xrightarrow{\mathrm{GOx}} \mathrm{Gluconic\ Acid} + \mathrm{H_2O_2} \tag{4}$$

$$\mathrm{Histamine} + \mathrm{H_2O} \xrightarrow{\mathrm{DAO}} \mathrm{ImAA} + \mathrm{NH_3} + \mathrm{H_2O_2} \tag{5}$$

where GOx and DAO represent glucose oxidase and diamine oxidase, respectively, and ImAA stands for imidazole acetic acid. Glucose is the essential substance in terms of metabolism; the glucose concentration in the blood is an efficient indicator for follow-up examination of diabetes. Another example is histamine, a biogenic neurotransmitter. It can influence many cells' reactions, including allergy and inflammation. With sufficient ABTS and HRP, coupled enzymatic reactions can be formed by combining (1) with (4) and (5), respectively, and the absorbance of the materiel would be proportional to the concentration of glucose and histamine, respectively. Therefore, the ABTS/H_2O_2/HRP method is quite useful to quantitate these targets' concentration for medical diagnosis.

C. Preparation of Biochemical Reagents

ABTS (10 mg/tab), H_2O_2 (30%, W/W), HRP (250 U/mg), β-D-glucose, histamine, and DAO from porcine kidney (0.06 U/mg) were purchased from Sigma. GOx from Aspergillus niger was purchased from Fluka. Sodium phosphate powders (monobasic and dibasic) were obtained from J. T. Baker. Other chemical reagents were of analytical grade and were used without further purification.

The HRP, GOx, and DAO stock solutions were prepared in a 100-mM phosphate buffer and were stored at $-20°C$. These stock enzyme solutions were melted in an ice bath just before use and were diluted with a pH 7.0 phosphate buffer. The activity assays of HRP, GOx/HRP, and DAO/HRP in the systems containing various concentrations of H_2O_2, glucose, and histamine, respectively, were initiated by adding 1-ml colorimetry reagent (30-mM ABTS in a 100-mM phosphate buffer, pH 7.0). The reactions were performed at 25°C (for HRP and GOx/HRP) and 37°C (for HRP and DAO/HRP), respectively.

D. CMOS Biochip

Referring to Fig. 1, the CMOS biochip was mainly composed of a photodetector and a TIA. Fig. 2 depicts the top view and cross section of the proposed P^+/N_{well} finger photodiode. Typically, a CMOS photodiode can be formed by adopting a N_{well}/P_{sub}, N^+/P_{well}, or P^+/N_{well} junction. With the illumination of the short wavelength light for biochemical experiments, the absorption depth of silicon is quite shallow, and most photogenerated carriers are very close to the photodiode surface. Since only the excess carriers inside the depletion region and within the diffusion length contribute to the photocurrent, the shallower P^+/N_{well} junction (about 0.2-μm deep) was adopted in this study to accomplish a better responsivity. (N^+/P_{well} junction is an alternative.) Moreover, the interdigitated P^+/N_{well} junctions was used to extend the depletion regions near the surface and, hence, increase the

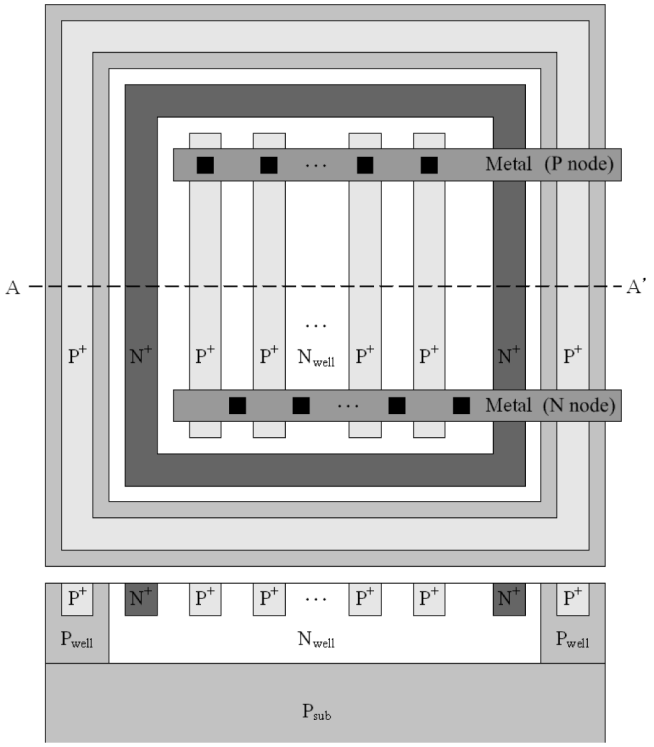

Fig. 2. The top view and cross section of $rmP^+/\mathrm{N_{well}}$ finger photodiode.

photocurrent [15]. Each P^+ stripe was 1-μm wide with 4-μm spacing, and the stripes were interconnected by metal lines and contacts. The total area of this finger photodiode was 100 μm$\times$ 100 μm. The photodiode was surrounded by double guard rings to keep the substrate noise off; the P^+ guard ring was connected to ground, and the N^+ guard ring was connected to a high potential [16].

In a standard CMOS technology, the dielectric layers above the active region comprise an interlayer dielectric layer, intermetal dielectric layers, and optional passivation layers (PASS). For a multilayer structure, the reflectance can be calculated by using the impedance-transformation approach. The effective wave impedance Z_i at the front of the ith layer is expressed as [17]

$$Z_i = \eta_i \frac{Z_{i+1} + j\eta_i \tan(k_i d_i)}{\eta_i + jZ_{i+1}\tan(k_i d_i)} \tag{6}$$

where η_i, k_i, and d_i denote the intrinsic impedance, the wavenumber, and the thickness of the ith layer, respectively; Z_{i+1} denotes the effective impedance at the front of the $(i+1)$th layer. This recursive calculation starts from the known impedance of the last layer (silicon substrate), $Z_{\mathrm{last}} = \eta_{\mathrm{Si}}$, backward to the effective impedance at the front of the surface layer, Z_1. Then, the reflectance R of the photodiode can be obtained as

$$R = \left| \left(\frac{Z_1 - \eta_0}{Z_1 + \eta_0} \right)^2 \right| \tag{7}$$

where η_0 is the intrinsic impedance of air. For the device with and without PASS, the simulation results of the wavelength-dependent reflectance are shown in Fig. 3. By removing PASS above the active region of the photodiode, it shows that the reflectance can be reduced from 0.169 to 0.116 for the 430-nm light, and from 0.481 to 0.006 for the 650-nm light.

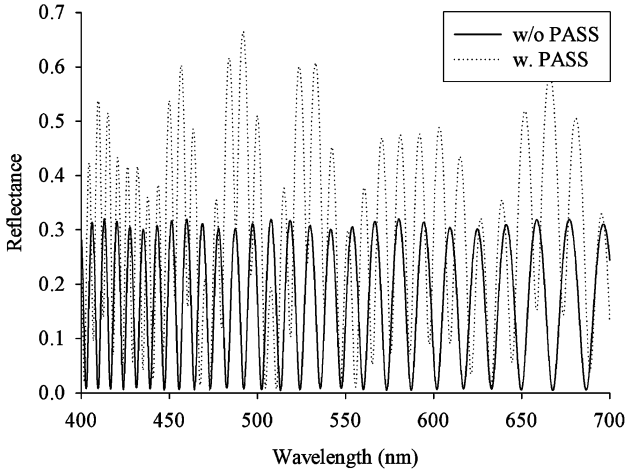

Fig. 3. The calculated reflectance as a function of wavelength for the device with and without passivation layers.

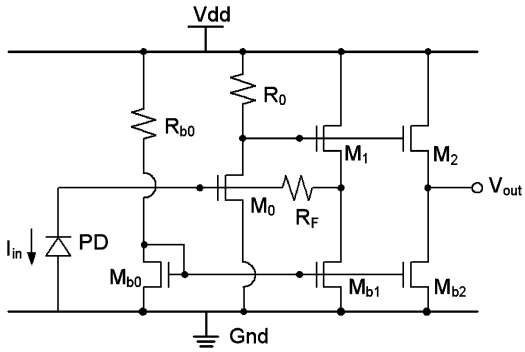

Fig. 4. The configuration of the subsequent circuits. Device parameters are $M_0 = (100\ \mu\mathrm{m}/0.5\ \mu\mathrm{m})$, $M_1 = M_2 = (50\ \mu\mathrm{m}/0.5\ \mu\mathrm{m})$, $M_{b0} = M_{b1} = M_{b2} = (1\ \mu\mathrm{m}/0.5\ \mu\mathrm{m})$, $R_0 = 8\ \mathrm{k}\Omega$, and $R_{b0} = 15\ \mathrm{k}\Omega$.

As shown in Fig. 4, the subsequent circuits included a current source, current mirrors, a TIA, and output buffers. The TIA consisted of a common-source stage M_0, two source followers M_1 and M_2, and an external feedback resistance R_F. M_1 served in the feedback loop to isolate R_0 from the loading effect, and M_2 drove the load capacitance to alleviate the stability issue [18]. The gain of the TIA is given as

$$A_T = \frac{R_F g_{m0} R_0}{1 + \frac{(R_F g_{m0} R_0)}{R_F}} \simeq R_F, \text{ for } g_{m0}R_0 \gg 1 \tag{8}$$

where g_{m0} is the transconductance of M_0; $g_{m0}R_0$ was designed large enough to make A_T approximated to R_F. The external R_F allowed us to adjust the amplification factor and the dynamic range of the TIA. The input-referred noise current of the TIA is given as

$$\overline{I_{n,in}^2} = \frac{4kT}{R_F} + \frac{4kT}{R_F^2}\left(\frac{\gamma}{g_{m0}} + \frac{1}{g_{m0}^2 R_0} + \frac{\gamma}{g_{m0}^2 g_{m1} R_0^2} \right) \tag{9}$$

where g_{m1} is the transconductance of M_1, and γ is the excess noise coefficient [18]. The input-referred noise current were reduced by enlarging g_{m0}, g_{m1}, R_0, and R_F. In addition, to prevent the abovementioned circuits from illumination, these regions were covered with floating metals as optical masks.

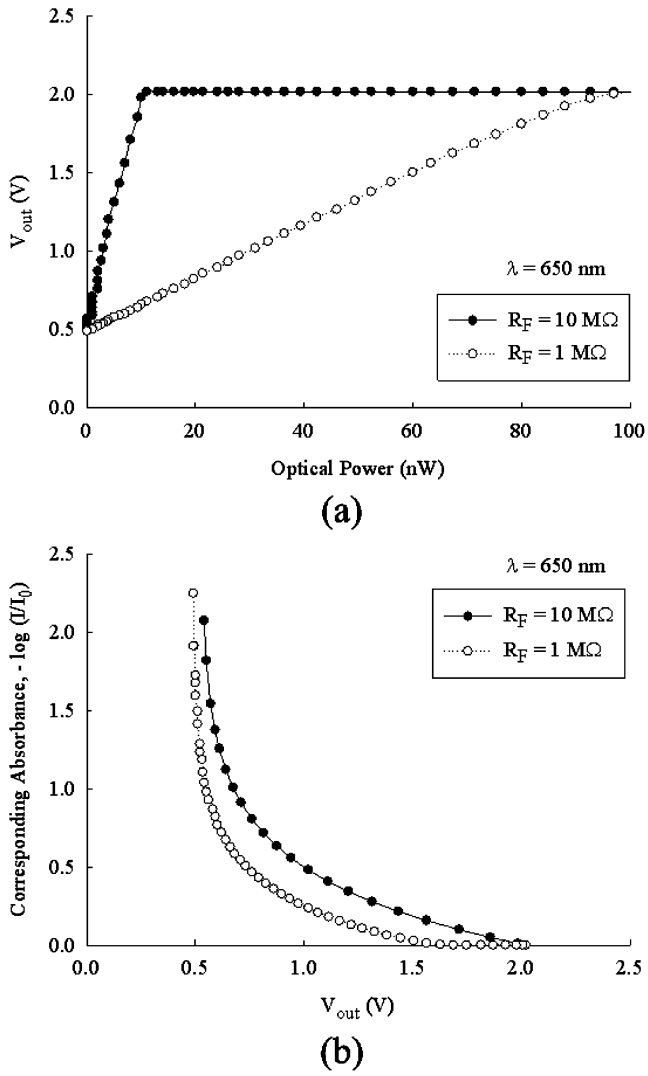

Fig. 5. Experimental results of the CMOS optical biosensing system with $R_F = 10$ MΩ and $R_F = 1$ MΩ at $\lambda = 650$ nm. (a) The output voltage versus the input optical power. (b) The corresponding absorbance versus the output voltage.

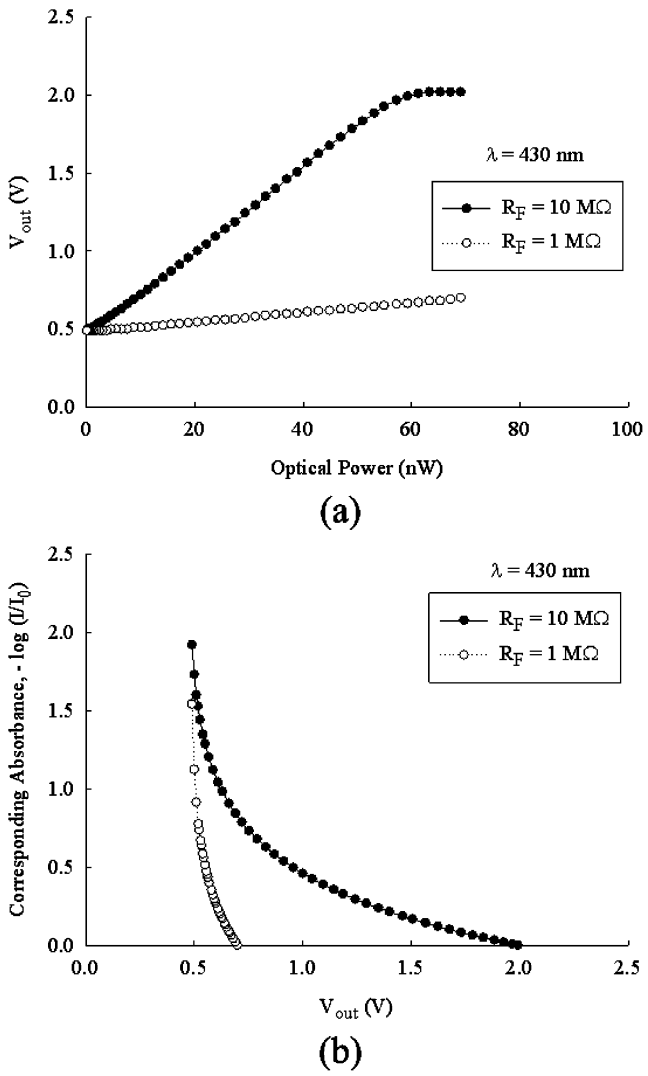

Fig. 6. Experimental results of the CMOS optical biosensing system with $R_F = 10$ MΩ and $R_F = 1$ MΩ at $\lambda = 430$ nm. (a) The output voltage versus the input optical power. (b) The corresponding absorbance versus the output voltage.

III. Experimental Results

A. Characteristics of the Whole System

The biochip was manufactured using the TSMC (Taiwan Semiconductor Manufacturing Company) 0.35-μm CMOS technology. The die size (including the photodiode, core circuits, and I/O pads) is 1.35 mm × 1.35 mm, and the dimensions of the miniature biosensing system shown in Fig. 1 are about 8 cm (length) × 6 cm (width) × 7 cm (height). The finger photodiode is reverse-biased moderately to ensure that the photocurrent is linearly proportional to the absorbed photons. The photocurrent is then converted into voltage signal by the subsequent TIA. With a 3-V power supply, the lower bound and upper bound of the output voltage are 0.49 and 2.02 V, respectively.

Red LEDs (Centenary 31134) and a bandpass filter (Onset 650FS10–50) are used to produce 650-nm light. When the biochip is illuminated, the output voltage $V_{\rm out}$ as a function of the input optical power for a 650-nm wavelength is shown in Fig. 5(a). For $R_F = 10$ MΩ and 1 MΩ, the sensitivities are approximately 145 V/μW and 16 V/μW, respectively. However, the output voltage $V_{\rm out}$ for $R_F = 10$ MΩ would saturate at 2.02 V when the input optical power is larger than 10 nW. Combining the results of the linear region with (2) gives the corresponding relationships between the absorbances and the output voltages for two different R_F's, as shown in Fig. 5(b). These relationships would be beneficial for the analysis of biochemical experiments since the absorbance of the material is proportional to the target's concentration.

Similarly, purple LEDs (Centenary 40327) and a bandpass filter (Newport 20BPF10–430) are used to produce 430-nm light. When the biochip is illuminated, the output voltage as a function of the input optical power for a 430-nm wavelength is shown in Fig. 6(a). For $R_F = 10$ MΩ and 1 MΩ, the sensitivities are approximately 26 V/μW and 3 V/μW, respectively. The output voltage $V_{\rm out}$ for $R_F = 10$ MΩ would saturate at 2.02 V when the input optical power is larger than 60 nW. The relationships between the absorbances and the output voltages for two different R_F's are shown in Fig. 6(b).

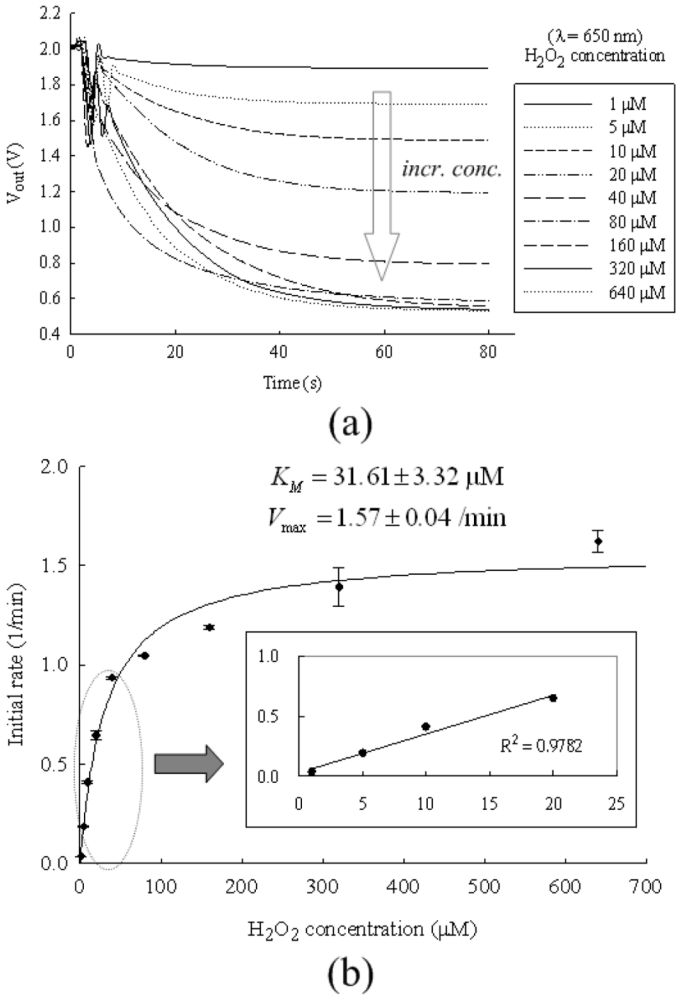

Fig. 7. Experimental results of the H_2O_2 detection with 650-nm light at 25 °C. (a) Real-time measurement of the output voltage for $t = 0-80$ s. (b) The Michaelis-Menten plot.

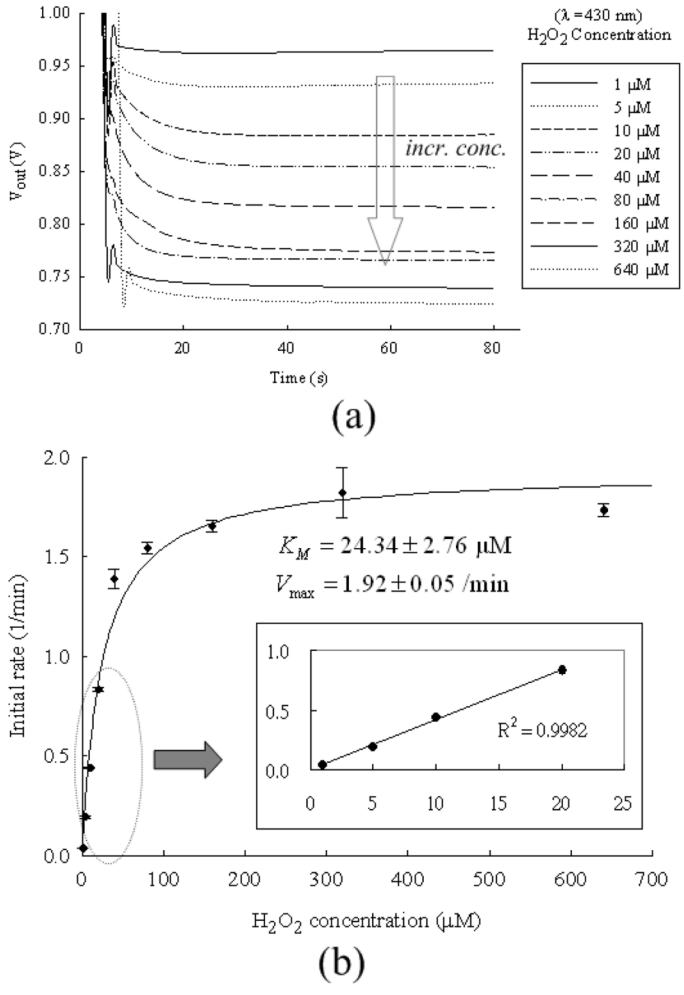

Fig. 8. Experimental results of the H_2O_2 detection with 430-nm light at 37 °C. (a) Real-time measurement of the output voltage for $t = 0-80$ s. (b) The Michaelis–Menten plot.

The measurement results of the CMOS chip indicate that the sensitivity of 650-nm light is higher than that of 430-nm light. But from the perspective on the biochemical product $ABTS^+$, the absorption of 430-nm light is stronger than that of 650-nm light. Accordingly, for comparison, the following biochemical experiments are performed with 650-nm light and 430-nm light individually.

B. H_2O_2 *Detection*

The biochemical equation of the ABTS/H_2O_2/HRP method is expressed in (1). When the substrate ABTS and the enzyme HRP are sufficient, the amount of the product $ABTS^+$ would be proportional to the H_2O_2 concentration. For the experiment performed using 650-nm light and $R_F = 1$ MΩ, Fig. 7(a) illustrates the real-time measured voltages V_{out} under various H_2O_2 concentration, with an arrow indicating the trend of increasing concentration (incr. conc.). The minimum H_2O_2 concentration was successfully detected as 1 μM, which is one order of magnitude better than the limit reported in previous literatures (about 50 μM) [1], [2], and is even comparable to the limit obtained from a commercial spectrophotometer (Hitachi U-3310). With the relationship depicted in Fig. 5(b), the absorbance at each time point for various H_2O_2 concentration can be obtained. The Michaelis-Menten plot of H_2O_2 concentration is shown in Fig. 7(b), where the Michaelis constant $K_m = 20.22 \pm 3.31$ μm is computed by using a nonlinear regression program (SigmaPlot). For a small $[H_2O_2]$, the experimental results demonstrate a good linearity with the coefficient of determination $R^2 = 0.9782$, as shown in the inset of Fig. 7(b).

Similarly, for the experiment performed using 430-nm light and $R_F = 10$ MΩ, Fig. 7(a) illustrates the real-time measured voltages V_{out} under various H_2O_2 concentration. The minimum H_2O_2 concentration was successfully detected also as 1 μM. With the relationship depicted in Fig. 5(b), the absorbance at each time point for various H_2O_2 concentration can be obtained. The Michaelis–Menten plot of H_2O_2 concentration is shown in Fig. 7(b), where $K_m = 22.28 \pm 6.61$ μM. For a small $[H_2O_2]$, the experimental results demonstrate a good linearity with $R^2 = 0.9982$ as shown in the inset of Fig. 7(b).

C. Glucose Detection

The coupled enzymatic reactions for glucose detection are expressed in (1) and (4). Sufficient ABTS, HRP, and GOx would ensure that the absorbance of the material is proportional to the glucose concentration. For the experiment performed using

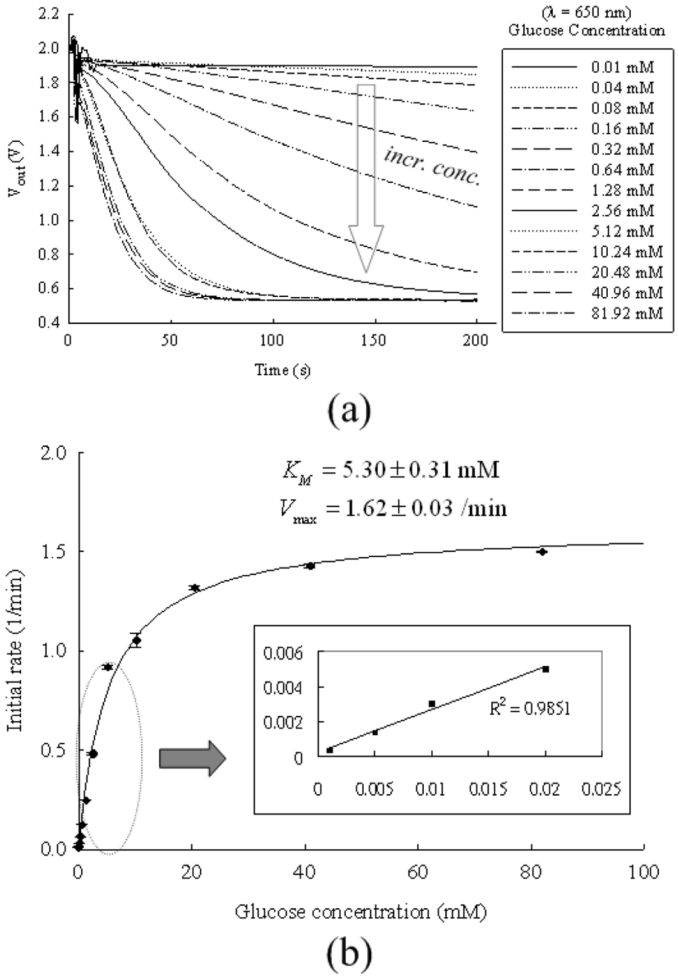

Fig. 9. Experimental results of the glucose detection with 650-nm light at 25 °C. (a) Real-time measurement of the output voltage for $t = 0-200$ s. (b) The Michaelis–Menten plot.

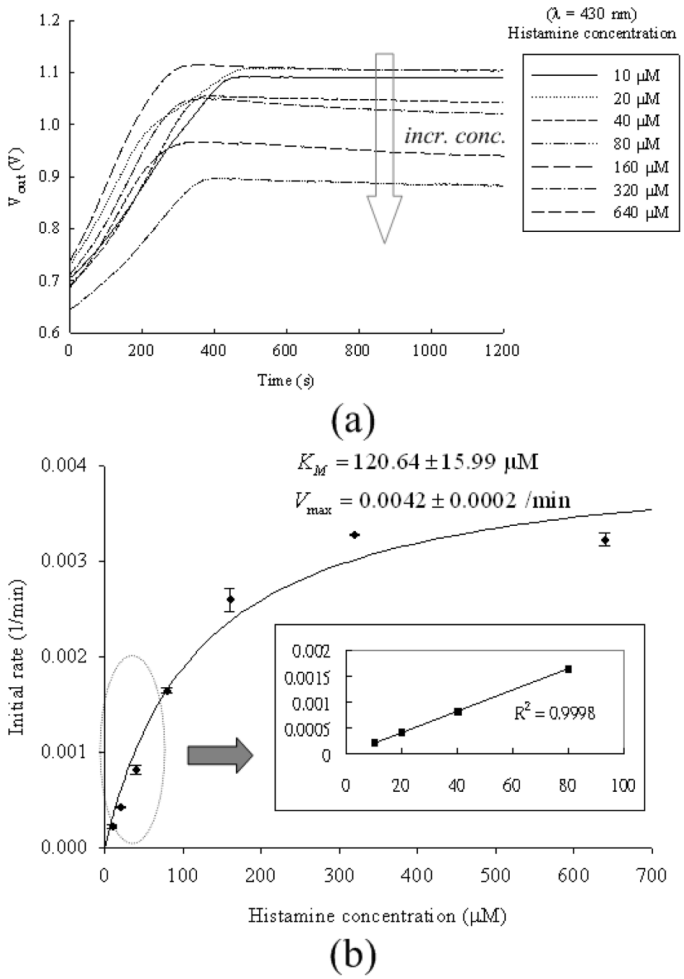

Fig. 10. Experimental results of the histamine detection with 430-nm light at 37 °C. (a) Real-time measurement of the output voltage for $t = 0-1200$ s. (b) The Michaelis–Menten plot.

650-nm light and $R_F = 1$ MΩ, the real-time measured voltages V_{out} under various glucose concentrations are illustrated in Fig. 9(a). The minimum glucose concentration was successfully detected as 10 μM. The Michaelis–Menten plot of glucose concentration is shown in Fig. 9(b), where $K_m = 4.87 \pm 0.99$ mM. In order to detect a lower glucose concentration, the experiment was then performed using $R_F = 10$ MΩ. The obtained Michaelis–Menten plot is shown in the inset of Fig. 9(b), where $R^2 = 0.9969$, and the detection limit of the glucose concentration was improved to 1 μM. This detection limit is two orders of magnitude better than the limit reported in previous literatures (about 500 μM) [1], [2], and is comparable to the limit obtained from a commercial spectrophotometer (Hitachi U-3310).

D. Histamine Detection

The coupled enzymatic reactions for histamine detection are expressed in (1) and (5). Sufficient ABTS, HRP, and DAO would ensure that the absorbance of the material is proportional to the histamine concentration. For the experiment performed using 430-nm light and $R_F = 10$ MΩ, the real-time measured voltages V_{out} under various histamine concentrations are illustrated in Fig. 10(a). The minimum histamine concentration was successfully detected as 10 μM, which is comparable to the limit obtained from a commercial spectrophotometer (Hitachi U-3310). The Michaelis–Menten plot of histamine concentration is shown in Fig. 10(b), where $K_m = 125.04 \pm 30.17$ μM. For a diluted histamine solution, the experimental results demonstrate a good linearity with $R^2 = 0.9877$, as shown in the inset of Fig. 10(b).

E. Interfering Agents

For the ABTS/H_2O_2/HRP system, although HRP, GOx, and DAO are highly specific enzymes, some chemicals in the blood may affect the H_2O_2 detection. Among the possible interfering agents in the blood, uric acid and acetaminophen were observed to have limited effects on the H_2O_2 detection, whereas ascorbic acid (AA) would somewhat affect the H_2O_2 detection [19]. For healthy adults, the physiological concentration of AA in the blood is about 60 μM, and the glucose concentration in the blood is about 3–8 mM [20], i.e., the ratio of [AA] to $[H_2O_2]$ is about 0.01. Since the sensitivity of our system for glucose detection is in the low μm range, the blood sample could be diluted to a 10^{-2} to 10^{-3} concentration for detection.

To investigate the effects of AA upon the ABTS/H_2O_2/HRP system, the experiments were performed using 10 μm H_2O_2 and various AA concentrations in the reaction mixture. The activity

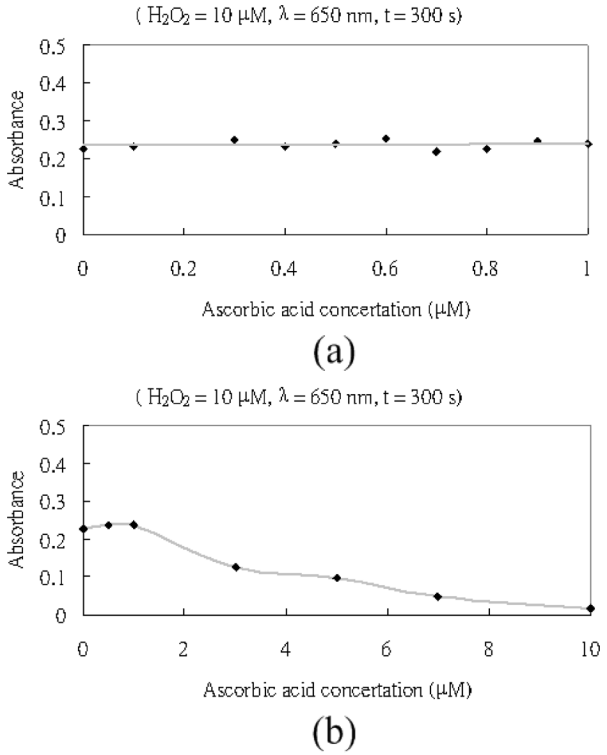

Fig. 11. The absorbance A of the reaction mixture versus the AA concentration. (a) At low concentration. (b) At high concentration.

of HRP was determined using the system with 650-nm light and $R_F = 1\ \mathrm{M}\Omega$, and the experimental results are shown in Fig. 11. For $[\mathrm{H_2O_2}] = 10\ \mu$m and $[\mathrm{AA}] < 1\ \mu$M, the variation in the absorbance A of the reaction mixture was negligible. For $[\mathrm{H_2O_2}] = 10\ \mu$m and $[\mathrm{AA}] > 3\ \mu$M, the significant interference with the ABTS/$\mathrm{H_2O_2}$/HRP system due to the large AA concentration can be observed. However, when the diluted blood sample of a healthy adult is used in our detection system, the ratio of [AA] to $[\mathrm{H_2O_2}]$ is about 0.01 and the expected AA concentration is much less than 1 μM. Therefore, the interference from AA is also negligible for the blood examination.

IV. Conclusion

An optical biosensing system based on a standard CMOS technology and absorption photometry has been presented. The whole system was assembled into a compact prototype, in which the CMOS biochip composed of a photodiode and a TIA demonstrated a high sensitivity and linearity. The quantum efficiency of the $\mathrm{P^+/N_{well}}$ photodiode was enhanced by adopting the interdigitated structure and removing the passivation layers in the CMOS structure. In addition, the switchable feedback resistance of the TIA allowed a user to adjust the amplification factor and the dynamic range for examining different concentration levels of an analyte. The ABTS/$\mathrm{H_2O_2}$/HRP method was introduced as a useful basis for quantifying various analytes by coupling them with biochemical reactions that produce $\mathrm{H_2O_2}$. The experimental results reveal that the detection limits of $\mathrm{H_2O_2}$, glucose, and histamine concentration are 1 μM, 1 μM, and 10 μM, respectively. The detection limits are at least one order of magnitude better than those of reported CMOS biosensors, and are even comparable to those of a commercial spectrophotometer.

The whole system exhibits a high detection capability, a large dynamic range, a high reproducibility, a short response time, and a low sample volume requirement. Therefore, the development of this CMOS biosensing system is a stepping stone toward a portable, reliable, inexpensive, and convenient home care instruments. In the future, more advanced functions such as rapid screening and automatic monitoring could be realized, and a practical miniature instrument for personalized clinical diagnosis may be reasonably expected.

Acknowledgment

The authors would like to thank CIC for the assistance in chip manufacture and Yu-Ting Tai for the support of ascorbic acid experiments.

References

[1] W.-J. Ho, J.-S. Chen, M.-D. Ker, T.-K. Wu, C.-Y. Wu, Y.-S. Yang, Y.-K. Li, and C.-J. Yuan, "Fabrication of a miniature CMOS-based optical biosensor," *Biosens. Bioelectron.*, vol. 22, pp. 3008–3013, 2007.

[2] U. Lu, B. C.-P. Hu, Y.-C. Shih, C.-Y. Wu, and Y.-S. Yang, "The design of a novel complementary metal oxide semiconductor detection system for biochemical luminescence," *Biosens. Bioelectron.*, vol. 19, pp. 1185–1191, 2004.

[3] R. Eisenthal and M. J. Danson, *Enzyme Assays: A Practical Approach*, 2nd ed. Oxford, U.K.: Oxford Univ. Press, 2002.

[4] R. A. Yotter, L. A. Lee, and D. M. Wilson, "Sensor technologies for monitoring metabolic activity in single cells-part I: Optical methods," *IEEE Sensors J.*, vol. 4, pp. 395–411, 2004.

[5] U. Lu, B. C.-P. Hu, Y.-C. Shih, Y.-S. Yang, C.-Y. Wu, C.-J. Yuan, M.-D. Ker, T.-K. Wu, Y.-K Li, Y.-Z. Hsieh, W. Hsu, and C.-T. Lin, "CMOs chip as luminescent sensor for biochemical reactions," *IEEE Sensors J.*, vol. 3, pp. 310–316, 2003.

[6] R. A. Yotter and D. M. Wilson, "A review of photodetectors for sensing light-emitting reporters in biological systems," *IEEE Sensors J.*, vol. 3, pp. 288–303, 2003.

[7] V. P. Chodavarapu, D. O. Shubin, R. M. Bukowski, E. C. Tehan, A. H. Titus, A. N. Cartwright, and F. V. Bright, "CMOS-based biosensor systems using integrated nanostructured recognition elements," in *Proc. SPIE*, 2006, vol. 6095, pp. 126–133.

[8] A. C. Pimentel, A. T. Pereira, V. Chu, D. M. F. Prazeres, and J. P. Conde, "Detection of chemiluminescence using an amorphous silicon photodiode," *IEEE Sensors J.*, vol. 7, pp. 415–416, Jul. 2007.

[9] S.-H. Huanga, Y.-C. Shih, C.-Y. Wu, C.-J. Yuan, Y.-S. Yang, Y.-K. Li, and T.-K. Wu, "Detection of serum uric acid using the optical polymeric enzyme biochip system," *Biosens. Bioelectron.*, vol. 19, pp. 1627–1633, 2004.

[10] S. Donati, *Photodetectors—Devices, Circuits, and Applications*. Englewood Cliffs, NJ: Prentice-Hall, 2000.

[11] Y.-W. Chang, P.-C. Yu, Y.-T. Huang, and Y.-S. Yang, "A CMOS-compatible optical biosensing system based on visible absorption spectroscopy," in *Proc. 2007 IEEE Int. Conf. Electron Devices and Solid-State Circuits*, 2007, vol. 2, pp. 1099–1102.

[12] R. Bourbonnais, D. Leech, and M. G. Paice, "Electrochemical analysis of the interactions of laccase mediators with lignin model compounds," *Biochimica et Biophysica Acta*, vol. 1379, pp. 381–390, 1998.

[13] P. N. Campbell, A. D. Smith, and T. J. Peters, *Biochemistry Illustrated:Biochemistry and Molecular Biology in the Post-Genomic Era*, 5th ed. New York: Elsevier, 2005.

[14] E. C. Webb, *Enzyme Nomenclature 1992*. New York: Academic, 1992.

[15] A. Ghazi, H. Zimmermann, and P. Seegebrecht, "CMOS photodiode with enhanced responsivity for the UV/blue spectral range," *IEEE Trans. Electron Devices*, vol. 49, pp. 1124–1128, 2002.

[16] M.-D. Ker and W.-Y. Lo, "Methodology on extracting compact layout rules for latchup prevention in deep-submicron bulk CMOS technology," *IEEE Trans. Semicond. Manuf.*, vol. 16, pp. 319–334, 2003.

[17] D. K. Cheng, *Field and Wave Electronmagnetics*. Reading, MA: Addison-Wesley, 1989.

[18] B. Razavi, *Design of Integrated Circuits for Optical Communications*. New York: McGraw-Hill, 2003.

[19] L. Zhu, R. Yang, J. Zhai, and C. Tian, "Bienzymatic glucose biosensor based on co-immobilization of peroxidase and glucose oxidase on a carbon nanotubes electrode," *Biosens. Bioelectron.*, vol. 23, pp. 528–535, 2007.

[20] D. L. Sherman, J. F. Keaney, E. S. Biegelsen, S. J. Duffy, J. D. Coffman, and J. A. Vita, "Pharmacological concentrations of ascorbic acid are required for the beneficial effect on endothelial vasomotor function in hypertension," *J. American Heart Association*, vol. 35, pp. 936–941, 2000.

Yu-Wei Chang was born in Taichung, Taiwan, on March 9, 1980. He received the B.S. degree in electronics engineering from National Chiao Tung University (NCTU), Hsinchu, Taiwan, in 2002, and the M.S. degree in biophotonics engineering from National Yang Ming University, Taipei, Taiwan, in 2004. He is currently working towards the Ph.D. degree at the Institute of Electronics, NCTU.

His research interests include optoelectronic devices and integrated circuits for applications in high-speed networks and biomedical diagnosis.

Mr. Chang is a member of the Phi Tau Phi Scholastic Honor Society.

Ping-Chun Yu was born in Taipei, Taiwan, in 1975. He received the B.S. degree in mathematics from National Taiwan Normal University, Taipei, in 1998, and the M.S. degree in applied science and technology from National Chiao Tung University, Hsinchu, Taiwan, in 2008.

His research interests include biochemistry and biosensor.

Yang-Tung Huang (M'90) was born in Taiwan, in 1955. He received the B.S. degree in electrophysics, the M.S. degree in electronics from National Chiao Tung University, Taipei, Taiwan, in 1978 and 1982 respectively, and the Ph.D. degree in electrical and computer engineering (minor in optical sciences) from the University of Arizona, Tucson, in 1990.

He is a Professor with the Department of Electronics Engineering and the Institute of Electronics, and a Joint Professor at the Department of Biological Science and Technology, National Chiao Tung University. He has been the Director of the Institute of Electronics for three years, the Director of Semiconductor Research Center for two years, and the Director of Nano Facility Center for four years. His current researches include integrated optics, photonic crystal waveguides, bio-optoelectronics, and optoelectronic switching networks.

Prof. Huang received the Outstanding Research Award from the National Science Council in 1998.

Yuh-Shyong Yang received the B.S. degree in forestry from National Taiwan University, Taipei, the M.S. degree in wood science and technology from the University of California, Berkeley, and the Ph.D. degree in biochemistry from the University of Wisconsin, Madison, in 1979, 1983, and 1987, respectively.

He is currently a Professor with the Department of Biological Science and Technology, National Chiao Tung University, and an Adjunct Research Fellow at the Instrument Technology Research Center and National Nano Device Laboratories, Taiwan. His research interests involve the interface between biochemistry and electronics. In particular, he is interested in the specific interactions of biomolecules and their effects on electronic responses from semiconductor devices.